

Optimizing Conical Intersections by Spin–Flip Density Functional Theory: Application to Ethylene

Noriyuki Minezawa and Mark S. Gordon*

Department of Chemistry, Iowa State University, Ames, Iowa 50011

Received: August 19, 2009; Revised Manuscript Received: October 8, 2009

Conical intersections (CIs) of ethylene have been successfully determined using spin-flip density functional theory (SFDF) combined with a penalty-constrained optimization method. We present in detail three structures, twisted-pyramidalized, hydrogen-migrated, and ethylidene CIs. In contrast to the linear response time-dependent density functional theory, which predicts a purely twisted geometry without pyramidalization as the S_1 global minimum, SFDF gives a pyramidalized structure. Therefore, this is the first correct optimization of CI points of twisted ethylene by the DFT method. The calculated energies and geometries are in good agreement with those obtained by the multireference configuration interaction (MR-CI) method and the multistate formulation of second-order multireference perturbation theory (MS-CASPT2).

Conical interactions (CIs)^{1–5} are well-known to play a vital role in photochemical reactions involving ultrafast dynamics on electronically excited states. Since they provide efficient relaxation pathways of photoexcited molecules, it is important to determine the CI points in order to elucidate the mechanisms of photochemical reactions. A minimum-energy CI (MECI) point can be located routinely by the state-averaged complete active space self-consistent field (SA-CASSCF) method because the analytical gradient and derivative coupling vectors are available to specify the CI seam. However, dynamic electron correlation effects are not taken into account at the SA-CASSCF level. Recently, Mori and Kato⁶ have formulated the analytic derivative coupling of the multistate second-order perturbation theory for the SA-CASSCF reference (MS-CASPT2) and pointed out the importance of dynamic electron correlation effects to evaluate potential energy surfaces and geometries at the MECI points.

Time-dependent density functional theory (TDDFT)^{7–9} is an alternative approach to take account of dynamic correlation effects for describing electronically excited states. Although TDDFT has been employed routinely to describe the excited-state properties of large molecular systems, its applicability to a CI search is problematic for several reasons. First, organic molecules at CI points are often described as biradicals, and thus, the application of single-reference theory is not appropriate. Ethylene, as a simple example, undergoes cis–trans isomerization in its excited states, and the CI points and relevant reaction dynamics have been extensively studied to explain the observed short excited-state lifetime.^{10–21} It has been predicted that at one of the CI points, the twisting of the CC double bond is accompanied by the pyramidalization of one CH₂ group. Linear response (LR) TDDFT with the B3LYP functional, however, predicts a purely twisted geometry without pyramidalization to be the S_1 global minimum, while all of the previous

calculations by the SA-CASSCF(4,7)¹³ (four electrons in seven orbitals), multireference configuration interaction (MR-CI),¹⁵ and MS-CASPT2²⁰ methods predict a twisted-pyramidalized structure. This is due to the fact that LR-TDDFT allows only single excitations from the $\pi_\alpha\pi_\beta$ ground state. The first and second excited states of twisted (D_{2d}) ethylene are Z and V valence states, which are described as a linear combination of the reference $\pi_\alpha\pi_\beta$ and doubly excited $\pi_\alpha^*\pi_\beta^*$ configurations. Therefore, the simplest CASSCF calculation would employ a (2,2) active space. Previous calculations have shown that the pyramidalization develops a sizable dipole moment (sudden polarization effect) and lowers the V state energy.^{14,15,20,22,23} Therefore, it is necessary to account for double excitation character of the V state to predict the correct CI between the ground and V states. The LR-TDDFT method, however, cannot model such a doubly excited configuration. As a result, it predicts a purely twisted (not pyramidal) structure. Second, in the vicinity of CI points, LR-TDDFT gives too rapid a change in the potential energy curves. In addition, the response state becomes lower in energy than the reference state. To circumvent these problems that are inherent in the LR-TDDFT method, Levine et al.²⁰ have suggested the possibility of a spin-flip TDDFT (or simply “SFDF”) approach^{24,25} to locate the CI points. The spin-flip approach has been applied successfully to calculate low-lying singlet and triplet states in biradicals.²⁶ In contrast to the conventional LR-TDDFT method, SFDF employs the triplet $\alpha\alpha(M_S = +1)$ state as the reference and allows only $\alpha \rightarrow \beta$ spin-flipped excitations. When the $\pi_\alpha\pi_\alpha^*$ triplet state of ethylene is selected as the reference, the doubly excited configuration $\pi_\alpha^*\pi_\beta^*$ is taken into account as a single spin-flip excitation. Furthermore, SFDF treats both the S_0 and S_1 states on an equal footing as the response states, while the S_0 state is always the reference state in LR-TDDFT.

The main purpose of the present study is to examine the accuracy of the SFDF method for predicting the energies and geometries of CI points. The penalty-constrained minimization approach^{20,21} is adopted to avoid computing the derivative

* To whom correspondence should be addressed. E-mail: mark@si.msg.chem.iastate.edu.

TABLE 1: Selected Geometrical Parameters at the Equilibrium and CI Points of Ethylene Obtained with SF-BHLYP/6-31G(d,p) (aug-cc-pVTZ)^a

	CC		CH		∠CCH	
(S ₀) _{min} (D _{2h})	1.327 (1.322)		1.077 (1.074)		121.7 (121.6)	
	C ₁ C ₂	C ₂ H ₅	C ₂ H ₆	∠C ₁ C ₂ H ₅	∠C ₁ C ₂ H ₆ (ω) ^b	θ ^c
twisted-pyr (PY)	1.383 (1.378)	1.098 (1.099)	1.142 (1.133)	114.1 (112.7)	89.3 (93.8)	65.9 (66.8)
H-migration (HM)	1.337 (1.336)	1.057 (1.055)	1.162 (1.160)	162.0 (161.8)	75.9 (77.1)	0.0 (0.3)
ethylidene (ET)	1.436 (1.434)	1.061 (1.060)		155.2 (156.1)		

^a Bond lengths are in angstroms, and angles are in degrees. Atom numbering is given in Figure 1 ^b Defined as the migration angle. ^c Pyramidalization angle θ defined as the out-of-plane angle from bond C₁C₂ to plane C₂H₅H₆.

TABLE 2: Relative Energies (in eV) at the Equilibrium and CI Points of Ethylene^a

		SF-BHLYP		MS-CASPT2 ^b	MR-CISD+Q ^c
		6-31G(d,p)	aug-cc-pVTZ	6-31G(d,p)	aug-cc-pVTZ
(S ₀) _{min}	1 ¹ A _g	0.00	0.00	0.00	0.00
	1 ¹ B _{1u}	8.35	7.67	8.67	7.80
twisted-pyr (PY)	1 ¹ A	4.84	4.71	4.81	4.50
	2 ¹ A	4.85	4.73	4.82	4.54
H-migration (HM)	1 ¹ A	5.47	5.28		5.17
	2 ¹ A	5.49	5.30		5.16
ethylidene (ET)	1 ¹ A	4.58	4.47	4.71	4.57
	2 ¹ A	4.60	4.49	4.73	4.56

^a Relative energies with respect to the ground-state minimum for the respective level of theory. ^b CIs are determined by the penalty constrained optimization, ref 21. ^c CIs are optimized by the analytical gradients and nonadiabatic coupling terms, ref 15.

coupling vectors. It is not trivial to obtain these vectors due to the lack of a wave function, although several methods have been proposed.^{27–30} The present study reports the successful location of the ethylene CI points using the SFDFD method combined with the penalty-constrained optimization method. Presented in detail are three structures, twisted-pyramidalized (PY), hydrogen-migrated (HM), and ethylidene (ET) CIs. The calculated energies and geometries are in good agreement with those obtained by the MR-CI¹⁵ and MS-CASPT2 methods.²¹

Within the original SFDFD formulation,^{24,31} the excitation energy Ω and transition amplitude X are obtained by solving the Hermitian matrix equation

$$\mathbf{AX} = \Omega\mathbf{X} \quad (1)$$

Only the spin-flipped block, that is, the αβ component, is allowed to be nonzero for the coupling matrix A and the transition amplitude X. The SFDFD coupling matrix A is given by

$$A_{ia,jb} = (\varepsilon_a - \varepsilon_i)\delta_{ij}\delta_{ab} - c_x \langle ial|jb \rangle \quad (2)$$

where *i* and *a* refer to occupied α and virtual β orbitals, respectively. {ε_{*i*}, ε_{*a*}} are the orbital energies obtained by solving the ground-state unrestricted Kohn–Sham equation for the αα (M_S = +1) triplet state, and c_x is a mixing weight of the Hartree–Fock exchange integral in the hybrid functional. In contrast to the conventional LR-TDDFT method, the Coulomb integrals, one of the exchange integrals, and the exchange–correlation kernel are zero due to the spin orthogonality.

In order to locate an intersection between states I and J, one minimizes the following objective function^{20,21}

$$f(\mathbf{R}, \sigma) = \frac{E_I(\mathbf{R}) + E_J(\mathbf{R})}{2} + \sigma \frac{[E_I(\mathbf{R}) - E_J(\mathbf{R})]^2}{E_I(\mathbf{R}) - E_J(\mathbf{R}) + \alpha} \quad (3)$$

where state I is taken to be the upper state. The α is a smoothing parameter to make eq 3 differentiable in the neighborhood of a

conical intersection, and σ is a Lagrange multiplier. The function *f* is minimized with fixed σ. If the resultant energy gap between the two states is larger than the threshold, σ is increased, and the optimization is restarted. The parameter σ is increased until the energy difference between the two states becomes less than the threshold. In other words, eq 3 optimizes the average energy of states I and J with the constraint that the energy gap between the two states is zero.

The SFDFD energy and analytic gradient were implemented in the electronic structure code GAMESS (General Atomic and Molecular Electronic Structure System).^{32,33} The BHLYP hybrid functional (50% Hartree–Fock plus 50% Becke exchange³⁴ with Lee–Yang–Parr correlation³⁵) was employed in this work because SFDFD benchmark calculations suggest better performance with a larger fraction of Hartree–Fock exchange.²⁴ The basis sets employed were 6-31G(d,p) and aug-cc-pVTZ.^{36,37} The former was used in the MS-CASPT2 study of ref 21 and the latter in the MR-CI calculations in ref 15. The Broyden–Fletcher–Goldfarb–Shannon (BFGS) quasi-Newton scheme was adopted to minimize the objective function in eq 3. The same optimization criteria, thresholds, and parameters were used as discussed in ref 21, where three criteria were considered to achieve convergence, the change in the objective function *f* and the parallel and perpendicular components of the gradient of *f* with respect to the direction of the gradient vector of the penalty (the second term in eq 3). They were minimized simultaneously to be lower than a given threshold. No symmetry constraint was applied during the CI optimizations.

The three CIs were successfully located by the SFDFD method and may be compared with the calculated energies and geometries obtained by the SA-CASSCF(2,2)/6-31G(d,p), MS-CASPT2/6-31G(d,p), and MR-CISD+Q/aug-cc-pVTZ (MR-CI) methods. The SA-CASSCF(2,2) and MS-CASPT2 methods employed the penalty-constrained MECI optimization ap-

proach,²¹ and the MR-CI CI points were determined using the analytic gradients and derivative coupling vectors in ref 15.

Only the lowest valence V ($^1B_{1u}$) state is considered here. Tables 1 and 2 summarize the optimized geometries for the ground state and the vertical excitation energies, respectively. The ground-state geometrical parameters are in reasonable agreement with those obtained by the MR-CI method,¹⁵ 1.337 Å, 1.083 Å, and 121.5° for the CC and CH bonds and the CCH angle, respectively. The vertical SF-BHLYP excitation energy, at the S_0 -optimized geometry, of the valence $N \rightarrow V$ ($^1A_g \rightarrow ^1B_{1u}$) transition is calculated to be 8.35 and 7.67 eV with the 6-31G(d,p) and aug-cc-pVTZ basis sets, respectively. These are comparable to the 8.67 and 7.80 eV obtained by MS-CASPT2/6-31G(d,p) and MR-CI/aug-cc-pVTZ, respectively. The SF-BHLYP/aug-cc-pVTZ vertical excitation energy is in very good agreement with the previously reported computational values^{13,15,38,39} and with the experimental absorption maximum of 7.66 eV⁴⁰ and the corrected value of 7.8 eV.⁴¹

Using SFDFT combined with the constrained optimization leads successfully to the three CI geometries, **PY**, **HM**, and **ET** (Figure 1). Special attention is paid to three geometrical parameters, the pyramidalization angle θ , which is defined as the out-of-plane angle from the C_1C_2 bond to the $C_2H_5H_6$ plane, the $C_1C_2H_6$ angle (ω) corresponding to the hydrogen migration, and the C_1C_2 bond length. For the **PY** geometry (Figure 1a), SF-BHLYP gives a correct pyramidalized CI in contrast to LR-TDDFT. As shown in Table 1, SF-BHLYP/6-31G(d,p) predicts $\theta = 66^\circ$ and $\omega = 89^\circ$, while MS-CASPT2 gives $\theta = 58^\circ$ and $\omega = 78^\circ$. Therefore, SF-BHLYP tends to underestimate the degree of migration. This may be attributed to spin contamination in the response states.⁴² Of the three CI structures, the **PY** has the largest spin contamination for the S_0 and S_1 states. The MS-CASPT2/6-31G(d,p) study illustrates that dynamic electron correlation affects the C_1C_2 bond of **PY**, 1.410 Å compared to the SA-CASSCF/6-31G(d,p) prediction of 1.386 Å. Interestingly, the SF-BHLYP/6-31G(d,p) value of 1.383 Å is close to the SA-CASSCF/6-31G(d,p) result.

The **HM** geometry (Figure 1b) has a planar $C_1C_2H_5H_6$ group ($\theta \sim 0^\circ$), and the symmetry of **HM** is nearly C_s with no symmetry constraint during the optimization. There is also a significant decrease in the distance between the migrating H_6 atom and the accepting C_1 atom, as well as the migration angle ω , 1.561 Å and 77.1° compared with 1.841 Å and 93.8° in the **PY** structure at the SF-BHLYP/aug-cc-pVTZ level. Note that the **HM** CI is not a true minimum on the crossing seam but rather a transition state along the path connecting the two equivalent **PY** forms.^{13–15}

In order to describe the **ET** species (Figure 1c), it is essential to employ a method (e.g., the SFDFT method) that can account for multireference character. Since **ET** has a carbene-like structure, a two-electron in two-orbital model is required to represent the three low-lying singlet states. SFDFT can treat these three states on an equal footing by spin-flip single excitations from the triplet carbene. The CC bond length of the **ET** structure is ~ 0.11 Å longer than that of the ground-state equilibrium geometry (1.327 Å). This elongation is not observed for the other two CI species. The **ET** structure is minimally dependent on the theoretical level, and the SFDFT-optimized geometry is in good agreement with those predicted by the MS-CASPT2 (MR-CI) calculations, 1.440 Å (1.448 Å) for the C_1C_2 bond length and 153.8° (155.1°) for the $C_1C_2H_5$ angle.

Now, consider the CI energies predicted by the SF-BHLYP method (Table 2). At the CI geometries, the energy gap between the two states in each structure is very small, less than 0.02

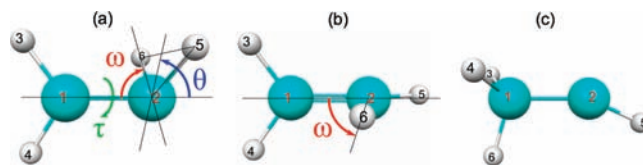


Figure 1. Geometries for the CIs of ethylene: (a) twisted-pyramidalized (**PY**), (b) hydrogen migration (**HM**), and (c) ethylidene (**ET**) CIs. Also shown are three important coordinates, the pyramidalization angle (θ), the H_6 migration angle (ω), and the twisting angle (τ).

eV; therefore, the average of the S_0 and S_1 CI energies is defined as the CI energy in the following discussion. The relative energies with respect to the ground-state minimum are in good agreement with those predicted by MS-CASPT2 and MR-CI, although the energetic order of the three CI points is slightly different. SF-BHLYP/aug-cc-pVTZ predicts **ET** to be lower in energy than the **PY** form by 0.24 eV, while MR-CISD predicts the **PY** and **ET** CIs to be isoenergetic. Nevertheless, both methods predict that the **HM** structure is higher in energy than the other two CI geometries. The energy difference between the **PY** and **HM** geometries is estimated to be 0.57 and 0.65 eV by the SF-BHLYP/aug-cc-pVTZ and MR-CI methods, respectively.

Finally, consider the behavior of the SF-BHLYP/6-31G(d,p) potential energy curves near the **PY** CI point. The twisting (τ) and H_6 migration (ω) angles (see Figure 1) were selected to distort the CI geometry, while all of the other geometrical parameters were fixed.⁴³ The SA-CASSCF(4,7) study by Ben-Nun and Martínez shows that the former coordinate corresponds approximately to the interstate nonadiabatic coupling vector and the latter to the gradient vector of the potential energy difference between the two states.¹³ These two vectors form a plane called the branching space, and the nuclear displacement in this plane lifts the degeneracy of the CI point.¹ For comparison, in the present work, potential energy surfaces were constructed with the SA-CASSCF(2,2)/6-31G(d,p) method, adopting the **PY** geometry in ref 21. Figure 2 compares the potential energy curves along the twisting ($\Delta\tau$) and $C_1C_2H_6$ angles ($\Delta\omega$) around the **PY** S_0/S_1 CI point. The SF-BHLYP/6-31G(d,p) curves (solid lines) are in qualitatively good agreement with those obtained by the SA-CASSCF(2,2)/6-31G(d,p) method (dashed lines). No rapid change in energy is observed for the SFDFT method. It is encouraging that SFDFT can provide qualitatively correct behavior of potential energy curves in the vicinity of a CI point. Therefore, it would be interesting to examine the applicability of the SFDFT method to CI points of large molecular systems.

The present study has applied the SFDFT method, combined with the penalty-constrained optimization method, to locate the CIs of ethylene. Three CI points have been successfully determined, **PY**, **HM**, and **ET**. The SFDFT is the first DFT-based method that gives the correct **PY** geometry; the LR-TDDFT gives a purely twisted structure without pyramidalization due to the lack of double excitation character. The energies and geometries are in good agreement with those obtained by the MR-CI and MS-CASPT2 methods.

The successful description of the CI structures by the SFDFT method is very promising. For example, it is interesting to describe the CIs of solvated molecules.^{18,44–48} The effective fragment potential (EFP) method⁴⁹ provides a polarizable force field to describe intermolecular interactions based on the ab initio methods. The energy and analytical gradient codes of the LR-TDDFT have been interfaced with the EFP method,^{50,51} and the extension to a SFDFT/EFP is straightforward. Another attractive

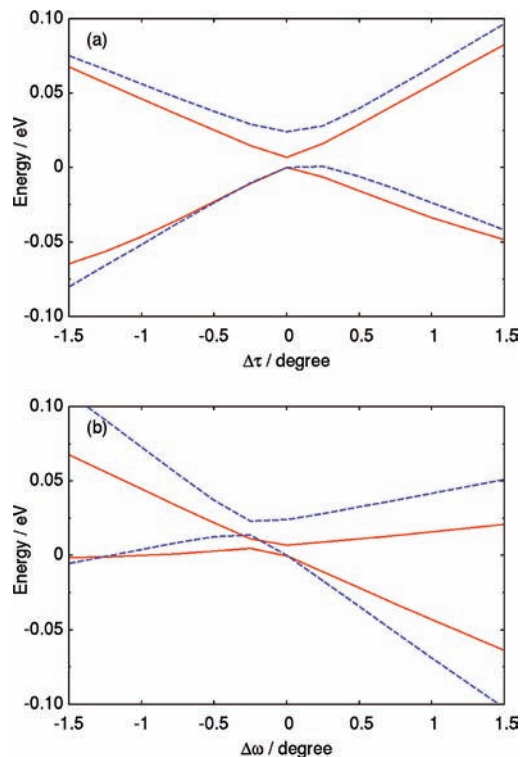


Figure 2. Behavior of SF-BHLYP/6-31G(d,p) (red solid lines) and SA-CASSCF(2,2)/6-31G(d,p) (blue dashed lines) potential energy curves near the twisted-pyramidalized CI (PY) in ethylene. The upper lines correspond to the S_1 state and the lower lines to the ground state. The distortion coordinates are the (a) twisting angle ($\Delta\tau$) and (b) $C_1C_2H_6$ migration angle ($\Delta\omega$). The ground-state energy at the CI point is the energy zero for the respective level of theory.

future direction is the nonadiabatic dynamics of photoexcited molecules. Several studies have been performed on the basis of TDDFT/nonadiabatic molecular dynamics.^{52–57} In order to combine the SFDFD with the nonadiabatic simulation, it is necessary to derive the nonadiabatic coupling elements within the framework of SFDFD. Although it is not trivial to define them because of the lack of a wave function in DFT-based methods, several approaches^{27–30} have been proposed and shown to be useful. Work is in progress along these lines.

Acknowledgment. This work was supported in part by a National Science Foundation Cyberinfrastructure grant and in part by a Department of Energy SciDAC grant, administered by the Ames Laboratory. The authors thank Professor Lyudmila Slipchenko for a careful reading of the manuscript and useful comments. Many enlightening discussions with Dr. Federico Zahariev are gratefully acknowledged.

Supporting Information Available: Cartesian coordinates for all geometries discussed in the text and energies for relevant electronic states. This material is available free of charge via the Internet at <http://pubs.acs.org>.

References and Notes

- Bernardi, F.; Olivucci, M.; Robb, M. A. *Chem. Soc. Rev.* **1996**, 25, 321.
- Levine, B. G.; Martínez, T. J. *Annu. Rev. Phys. Chem.* **2007**, 58, 613.
- Virshup, A. M.; Punwong, C.; Pogorelov, T. V.; Lindquist, B. A.; Ko, C.; Martínez, T. J. *J. Phys. Chem. B* **2009**, 113, 3280.
- Yarkony, D. R. *Acc. Chem. Res.* **1998**, 31, 511.
- Yarkony, D. R. *J. Phys. Chem. A* **2001**, 105, 6277.
- Mori, T.; Kato, S. *Chem. Phys. Lett.* **2009**, 476, 97.
- Runge, E.; Gross, E. K. U. *Phys. Rev. Lett.* **1984**, 52, 997.
- Casida, M. E. In *Recent Advances in Density Functional Methods*; Chong, D. P., Ed.; World Scientific: Singapore, 1995; Vol. 1, p 155.
- Burke, K.; Werschnik, J.; Gross, E. K. U. *J. Chem. Phys.* **2005**, 123, 062206.
- Ohmine, I. *J. Chem. Phys.* **1985**, 83, 2348.
- Freund, L.; Klessinger, M. *Int. J. Quantum Chem.* **1998**, 70, 1023.
- Ben-Nun, M.; Martínez, T. J. *Chem. Phys. Lett.* **1998**, 298, 57.
- Ben-Nun, M.; Martínez, T. J. *Chem. Phys.* **2000**, 259, 237.
- Krawczyk, R. P.; Viel, A.; Manthe, U.; Domcke, W. *J. Chem. Phys.* **2003**, 119, 1397.
- Barbatti, M.; Paier, J.; Lischka, H. *J. Chem. Phys.* **2004**, 121, 11614.
- Barbatti, M.; Granucci, G.; Persico, M.; Lischka, H. *Chem. Phys. Lett.* **2005**, 401, 276.
- Barbatti, M.; Ruckebauer, M.; Lischka, H. *J. Chem. Phys.* **2005**, 122, 174307.
- Yamazaki, S.; Kato, S. *J. Chem. Phys.* **2005**, 123, 114510.
- Levine, B. G.; Coe, J. D.; Virshup, A. M.; Martínez, T. J. *Chem. Phys.* **2008**, 347, 3.
- Levine, B. G.; Ko, C.; Quenneville, J.; Martínez, T. J. *Mol. Phys.* **2006**, 104, 1039.
- Levine, B. G.; Coe, J. D.; Martínez, T. J. *J. Phys. Chem. B* **2008**, 112, 405.
- Boorke, B. R.; Schaefer, H. F., III. *J. Am. Chem. Soc.* **1979**, 101, 307.
- Buenker, R. J.; Bonačić-Koutecký, V.; Pogliani, L. *J. Chem. Phys.* **1980**, 73, 1836.
- Shao, Y.; Head-Gordon, M.; Krylov, A. I. *J. Chem. Phys.* **2003**, 118, 4807.
- Wang, F.; Ziegler, T. *J. Chem. Phys.* **2004**, 121, 12191.
- Slipchenko, L. V.; Krylov, A. I. *J. Chem. Phys.* **2002**, 117, 4694.
- Chernyak, V.; Mukamel, S. *J. Chem. Phys.* **2000**, 112, 3572.
- Billeter, S. R.; Curioni, A. *J. Chem. Phys.* **2005**, 122, 034105.
- Hu, C.; Hirai, H.; Sugino, O. *J. Chem. Phys.* **2007**, 127, 064103.
- Tavernelli, I.; Tapavicza, E.; Rothlisberger, U. *J. Chem. Phys.* **2009**, 130, 124107.
- In ref 24, the SF-TDDFT method is introduced within the Tamm–Dancoff approximation (TDA), and the resultant SF-TDDFT/TDA is simply denoted as SF-DFT. However, it is not necessary to apply the TDA because the coupling matrix B is exactly zero as long as the conventional exchange-correlation functionals are employed. An exception is the noncollinear scheme for the exchange-correlation potential proposed in ref 25, which allows for spin-flip transitions and provides nonzero B matrix.
- Schmidt, M. W.; Baldrige, K. K.; Boatz, J. A.; Elbert, S. T.; Gordon, M. S.; Jensen, J. H.; Koseki, S.; Matsunaga, N.; Nguyen, K. A.; Su, S. J.; Windus, T. L.; Dupuis, M.; Montgomery, J. A., Jr. *J. Comput. Chem.* **1993**, 14, 1347.
- Gordon, M. S.; Schmidt, M. W. In *Theory and Applications of Computational Chemistry: the First Forty Years*; Dykstra, C. E., Frenking, G., Kim, K. S., Scuseria, G. E., Eds.; Elsevier: Amsterdam, The Netherlands, 2005; Chapter 41, pp 1167–1189.
- Becke, A. D. *Phys. Rev. A* **1988**, 38, 3098.
- Lee, C.; Yang, W.; Parr, R. G. *Phys. Rev. B* **1988**, 37, 785.
- Dunning, T. H., Jr. *J. Chem. Phys.* **1989**, 90, 1007.
- Kendall, R. A.; Dunning, T. H., Jr.; Harrison, R. J. *J. Chem. Phys.* **1992**, 96, 6796.
- Serrano-Andrés, L.; Merchán, M.; Nebot-Gil, I.; Lindh, R.; Roos, B. O. *J. Chem. Phys.* **1993**, 98, 3151.
- Müller, T.; Dallos, M.; Lischka, H. *J. Chem. Phys.* **1999**, 110, 7176.
- Wilkinson, P. G.; Mulliken, R. S. *J. Chem. Phys.* **1955**, 23, 1895.
- Petrongolo, C.; Buenker, R. J.; Peyerimhoff, S. D. *J. Chem. Phys.* **1982**, 76, 3655.
- The spin expectation values were evaluated by using the formula for the SF-CI singles, that is, the Kohn–Sham determinant was used instead of the Slater determinant. This is a crude approximation because there is no wavefunction in DFT.
- We restricted the motion of the H_6 atom in the $C_1C_2H_6$ plane of the CI geometry. Therefore, the dihedral angles of $H_3C_1C_2H_6$ and $H_4C_1C_2H_6$ are constant along the migration coordinate.
- Toniolo, A.; Granucci, G.; Martínez, T. J. *J. Phys. Chem. A* **2003**, 107, 3822.
- Toniolo, A.; Olsen, S.; Manohar, L.; Martínez, T. J. *Faraday Discuss.* **2004**, 127, 149.
- Burghardt, I.; Cederbaum, L. S.; Hynes, J. T. *Faraday Discuss.* **2004**, 127, 395.
- Spezia, R.; Burghardt, I.; Hynes, J. T. *Mol. Phys.* **2006**, 104, 903.
- Burghardt, I.; Hynes, J. T. *J. Phys. Chem. A* **2006**, 110, 11411.
- Gordon, M. S.; Freitag, M. A.; Bandyopadhyay, P.; Jensen, J. H.; Kairys, V.; Stevens, W. J. *J. Phys. Chem. A* **2001**, 105, 293.
- Yoo, S.; Zahariev, F.; Sok, S.; Gordon, M. S. *J. Chem. Phys.* **2008**, 129, 144112.

(51) Minezawa, N.; De Silva, N.; Zahariev, F.; Gordon, M. S. In preparation.

(52) Craig, C. F.; Duncan, W. R.; Prezhdo, O. V. *Phys. Rev. Lett.* **2005**, *95*, 163001.

(53) Tapavicza, E.; Tavernelli, I.; Rothlisberger, U. *Phys. Rev. Lett.* **2007**, *98*, 023001.

(54) Tapavicza, E.; Tavernelli, I.; Rothlisberger, U.; Filippi, C.; Casida, M. E. *J. Chem. Phys.* **2008**, *129*, 124108.

(55) Werner, U.; Mitrić, R.; Suzuki, T.; Bonačić-Koutecký, V. *Chem. Phys.* **2008**, *349*, 319.

(56) Mitrić, R.; Werner, U.; Bonačić-Koutecký, V. *J. Chem. Phys.* **2008**, *129*, 164118.

(57) Hirai, H.; Sugino, O. *Phys. Chem. Chem. Phys.* **2009**, *11*, 4570.

JP908032X